Statistical Characterization of the Spatiotemporal Variability of Soil Moisture and Vegetation in North America for Regional Climate Model Applications

Christopher L. Castro
Department of Atmospheric Sciences, University of Arizona
E-mail: castro@atmo.arizona.edu

Adriana Beltrán-Przekurat and Roger A. Pielke, Sr.
CIRES, University of Colorado at Boulder

Colorado
University of Colorado at Boulder

The University of Arizona
Tucson Arizona

1. Introduction

Our previous work has established that the dominant modes of Pacific sea surface temperatures (SSTs) influence the summer climate of North America via remote forcing of the large-scale circulation, or teleconnections. These teleconnections evolve in time and are most apparent during the early part of the summer, affecting the onset of the North American monsoon and the end to the late spring wet period in the central U.S. Our companion poster presented at this meeting summarizes how these teleconnections affect the physical mechanisms of summer rainfall within a regional climate model (RCM) framework. It has also been established via RCMs that the land surface influences of soil moisture and vegetation may significantly impact summer climate. However, these sensitivity-type studies have focused on only one or a few years, typically with extreme climate conditions like 1988 and 1993. The hypothesis posed here is that the land surface influences become more important during the latter part of the summer, when the influence of remote Pacific SST forcing diminishes. Our goal is to eventually test this hypothesis using a RCM as a complement to our previous work, with idealized land surface forcing corresponding to the statistically significant spatiotemporal patterns of soil moisture and vegetation. These must necessarily be "integrators" of longer-term atmospheric variability and may act synergistically with the summer teleconnections to create extreme climate conditions. The results presented herein show our initial statistical analysis of long-term North American precipitation, soil moisture and vegetation greenness datasets. The latter two products will be used to drive future idealized RCM simulations with the Regional Atmospheric Modeling System (RAMS).

2. Description of Soil Moisture and Vegetation Datasets

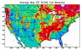

Figure 1: Climatological May soil moisture (unitless value as a fraction of saturation) from VIC model simulations.

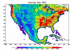

Figure 2: Climatological May NDVI (unitless) derived from AVHRR satellite data.

Soil moisture data is from a long-term integration of the Variable Infiltration Capacity (VIC) hydrologic model over the North American Land Data Assimilation System (NLDAS) domain at one-eighth degree resolution.

Vegetation greenness is defined using the Normalized Difference Vegetation Index (NDVI), available from GIMMS-NDVI data from 1981-present at 8 km resolution (Tucker et al. 2005). NDVI can be used to derive leaf area index (LAI) per RCM vegetation type with a transfer algorithm.

3. Statistical Analysis Methods

MTM-SVD Analysis: Allows for the detection and reconstruction of quasi-oscillatory spatio-temporal climate signals that exhibit episodes of spatially correlated behavior. Produces: 1) a local fractional variance (LFV) spectrum of the principal eigenmode; 2) statistical confidence intervals for the LFV spectrum; and 3) reconstructed anomaly patterns corresponding to the significant time-varying modes (e.g. Rajagopalan et al. 1998). The reference point for soil moisture and vegetation anomalies is defined as being in the central U.S. for the present analysis, unless otherwise specified.

Wavelet Analysis: Decomposes a time series into time/frequency space simultaneously, providing information on periodic signals and how these vary in time (Torrence and Compo 1998). Used here to confirm MTM-SVD analysis results by another method.

4. Dominant Spatiotemporal Modes of Global SST

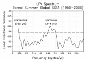

Figure 3: Principal eigenmode LFV spectrum of boreal summer global SST for 1950-2000. Dashed line indicates statistical significance at the 99% level. From Castro et al. (2006).

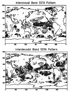

Figure 4: In-phase normalized SSTA associated with interannual and interdecadal bands, referenced to the eastern tropical Pacific. Values greater (less) than 1 (-1) shaded dark (light). Contour interval 0.25 units. From Castro et al. (2006).

Two statistically significant spatiotemporal modes of global SST are related to ENSO and ENSO-like decadal variability in the Pacific, at time scales of 3-4 years and about 22 years, respectively. The patterns shown here are for boreal summer, as this is the season that is of interest in our present work. These SST patterns are related to distinct atmospheric teleconnections in both warm and cold seasons, as shown for example on our companion poster and Castro et al. (2006). We therefore expect a priori that the statistically significant patterns of rainfall, soil moisture, and vegetation greenness would reflect the combination of SST forcing from both of these modes.

5. Standardized Precipitation Index (SPI)

The standardized precipitation index (SPI; McKee et al. 1993) normalizes a given precipitation total at each point to a gamma distribution, allowing for comparison of precipitation anomalies over varying climate regimes on a continental scale. In the present analysis, the one-month SPI is used for the CPC U.S.-Mexico long-term gauge-derived dataset (Higgins et al. 1996) for the period 1950-2002. The LFV spectrum for SPI considering all seasons (Fig. 5) shows significant interannual variability at a timescale of about seven years, which is the band of greatest interest here because significant variability in soil moisture and vegetation greenness occur at approximately the same time scale. This makes sense given that the most coherent patterns of atmospheric forcing, for both cold and warm seasons, occur when the interannual and interdecadal variability in the Pacific are in phase. The spatial pattern of variability reflects the well-established relationships between North American winter precipitation and ENSO/PDO in winter (Fig. 6). The corresponding wavelet analysis (Fig. 7) shows that the longer-term variability in central U.S. SPI is more dominant during the early part of the record and occurs at a slightly lower frequency.

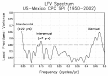

Figure 5: Principal eigenmode LFV spectrum of SPI for CPC U.S.-Mexico precipitation data (1950-2002). Dashed line indicates statistical significance at the 95% level.

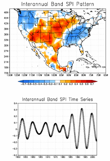

Figure 6: Spatial pattern (top) and time series (bottom) of in-phase SPI in the interannual band (unitless) referenced to the central U.S. for the period 1950-2002.

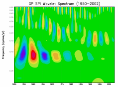

Figure 7: Wavelet spectrum of SPI (unitless) for an area encompassing the Great Plains for the period 1950-2002.

5. SPI Cold vs. Warm Season

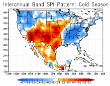

Figure 8: Same as Fig. 6 considering only the cold season (September to May).

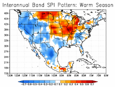

Figure 9: Same as Fig. 6 considering only the warm season (June to August).

A similar analysis of SPI in the interannual band considering total precipitation of the cold season (Fig. 8; September to May) and warm season (Fig. 9; June to August) separately reveals several additional important features of interannual precipitation variability. The cold season SPI pattern mirrors that for all seasons (Fig. 6), indicating that winter precipitation is likely more important than summer precipitation in determining drought conditions on interannual timescales. Central U.S. precipitation anomalies associated with interannual precipitation variability vary in the same way throughout the year. Therefore, the climate extremes in this region are very sensitive to the large-scale atmospheric forcing provided by Pacific SSTs. The most dramatic seasonal shift in the sign of precipitation anomalies associated with interannual variability occurs in the core monsoon region. This reflects the fact that interannual variability in winter versus summer precipitation is inversely related in this region. Therefore, a wet (dry) winter tends to be followed by a dry (wet) monsoon.

6. VIC NLDAS Soil Moisture

The statistically significant mode of interannual variability of VIC NLDAS soil moisture is at a slightly lower frequency than that of the SPI (Fig. 10). The largest anomalies in interannual soil moisture variability occur in the central U.S. (Fig. 11), and this is not surprising because the sign of interannual variation in precipitation there is consistent for the entire year (Figs. 8 and 9). The interannual band time series for soil moisture in the central U.S. (Fig. 11) matches the documented wet and dry periods there very well. In particular, long-term droughts occur at an approximately multidecadal frequency. In the observational record, these include the Dust Bowl of the mid-1930s, mid-1950s, mid-1970s, 1988-89, and the most recent drought of 1998-2002. We hypothesize that the most acute drought conditions in these periods are near the tail end of a cycle of relatively persistent Pacific SSTs, when the soil moisture deficit starts to act synergistically with atmospheric forcing (e.g. 1935-36, 1955-56, 1976-77, 2001-2002).

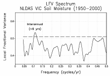

Figure 10: Principal eigenmode LFV spectrum of soil moisture for VIC NLDAS product (1950-2000). Dashed line indicates statistical significance at the 95% level.

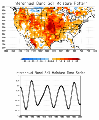

Figure 11: Spatial pattern (top) and time series (bottom) of in-phase VIC soil moisture anomalies in the interannual band (unitless) referenced to the central U.S. for the period 1950-2000.

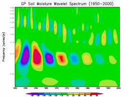

Figure 12: Wavelet spectrum of VIC soil moisture (unitless) for an area encompassing the Great Plains for the period 1950-2000.

7. Satellite-Derived NDVI

Significant interannual variability in AVHRR GIMMS-NDVI occurs on a timescale of about seven years (Fig. 13). Unlike soil moisture, long-term variability in vegetation greenness is a maximum in the southeast U.S. and does not correspond well with precipitation variability (Fig. 14). The likely reason for this is because vegetation growth is influenced by factors other than precipitation in this area. The surface temperature and availability of sunlight, and not moisture availability, may be the more dominant factors. Variability in vegetation greenness in the core monsoon region indicates a dependence on summer rainfall, especially west of the continental divide. We note there is a problem with NDVI data for 1994, which affect the NDVI time-series and wavelet analysis in Figs. 14 and 15. Also, the wavelet analysis is shown for the southeast U.S. instead of the central U.S. in this case.

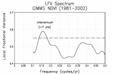

Figure 13: Principal eigenmode LFV spectrum of AVHRR GIMMS-NDVI (1981-2002). Dashed line indicates statistical significance at the 95% level.

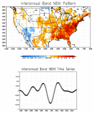

Figure 14: Spatial pattern (top) and time series (bottom) of in-phase AVHRR GIMMS-NDVI in the interannual band (unitless) referenced to the central U.S. for the period 1950-2000.

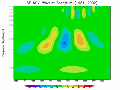

Figure 15: Wavelet spectrum of AVHRR GIMMS-NDVI (unitless) for an area encompassing the southeast U.S. for the period 1950-2000.

Acknowledgments: Research funded by NOAA grant NA67RJ0152 under NOAA CPPA-GAPP.